Acyl-Adenylate Motif of the Acyl-Adenylate/Thioester-Forming Enzyme Superfamily: A Site-Directed Mutagenesis Study with the *Pseudomonas* sp. Strain CBS3 4-Chlorobenzoate:Coenzyme A Ligase†

Kai-Hsuan Chang,‡ Hong Xiang, and Debra Dunaway-Mariano*

Department of Chemistry and Biochemistry, University of Maryland, College Park, Maryland 20742

Received May 28, 1997; Revised Manuscript Received September 8, 1997⊗

ABSTRACT: 4-Chlorobenzoate:coenzyme A (4-CBA:CoA) ligase catalyzes 4-chlorobenzoyl-coenzyme A formation in a two-step reaction consisting of the adenylation of 4-chlorobenzoate with adenosine 5′-triphosphate followed by acyl transfer from the 4-chlorobenzoyl adenosine 5′-monophosphate diester intermediate to coenzyme A. In this study, two core motifs present in the *Pseudomonas* sp. strain CBS3 4-CBA:CoA ligase (motif I, 161T-S-G-T-T-G-L-P-K-G170, and motif II, 302Y-G-T-T-E306) and conserved among the sequences representing the acyl-adenylate/thioester-forming enzyme family (to which the ligase belongs) were tested for their possible role in substrate binding and/or catalysis. The site-directed mutants G163I, G166I, P168A, K169M, and E306Q were prepared and then subjected to steady-state and transient kinetic studies. The results, which indicate reduced catalysis of the adenylation of 4-chlorobenzoate in the mutant enzymes, are interpreted within the context of the three-dimensional structure of the acyl-adenylate/thioester-forming enzyme family member, firefly luciferase.

4-Chlorobenzoate (4-CBA)[1] is degraded in special strains of bacteria via a three-step pathway (Scheme 1) which leads to 4-hydroxybenzoate, a metabolite that is ultimately processed through the aromatic *ortho* cleavage, β-ketoadipate and TCA pathways (for review see ref *1*).

The first step of the 4-CBA dehalogenation pathway is catalyzed by the enzyme 4-CBA:CoA ligase. This enzyme belongs to a large class of structurally related acyl-adenylate-forming enzymes (*2*, *3*). The enzymatic activities represented in this class include numerous acyl:CoA ligases (e.g., acetate:CoA ligase, fatty acid:CoA ligase, coumarate:CoA ligase, *O*-succinylbenzoate:CoA ligase, carnitine:CoA ligase, bile acid:CoA ligase, and benzoate:CoA ligase) for which the acyl-adenylate, formed by the reaction between the carboxylate substrate and ATP, serves as the intermediary acyl-donor to the thiol functionality of the CoA (Scheme 2) (*4*). The acyl-adenylate-forming domains of a number of large enzyme complexes that mediate the synthesis of peptide and polyketide secondary metabolites (e.g., gramicidin, tyrocidine, Aad-Cys-D-Val, enterobactin, and anguibactin) also belong to this family of enzymes. In these systems the acyl-adenylate formed serves as an acyl donor to an enzyme thiol residue (typically the thiol of an appended pantetheine), which in turn donates the acyl group to an amine or alcohol acceptor (Scheme 2) (for a recent review on these enzyme systems see ref *5*). Enzymes such as firefly luciferase and α-aminoadipate reductase, which catalyze otherwise seemingly unrelated reactions proceeding via acyl-adenylate intermediates (Scheme 2), are also members of this structural family (*3*). Luciferase is selectively activated by CoA,

Scheme 1: Chemical Steps of the 4-CBA to 4-HBA Pathway Catalyzed by 4-CBA:CoA Ligase, 4-CBA-CoA Dehalogenase, and 4-HBA-CoA Thioesterase (*2*)

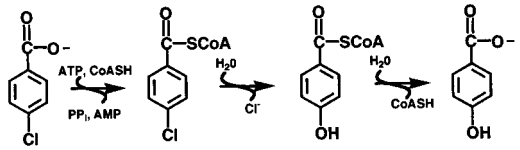

Scheme 2: Representation of the Types of Reactions Catalyzed by Enzymes of the Acyl-Adenylate/Thioester-Forming Enzyme Family

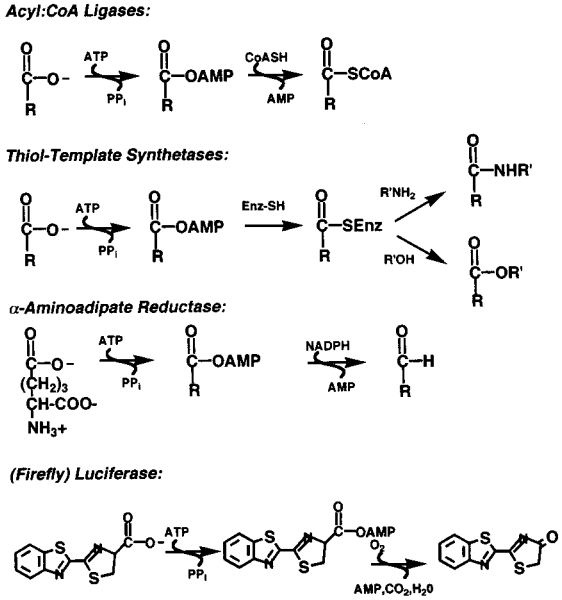

† This work was supported by NIH Grant GM 28688.

* To whom correspondence should be addressed at the Department of Chemistry, University of New Mexico, Albuquerque, NM 87131. Email: dd39@unm.edu

‡ Present address: Chiron, San Diego, CA.

⊗ Abstract published in *Advance ACS Abstracts,* December 1, 1997.

[1] Abbreviations: 4-CBA, 4-chlorobenzoate; 4-CBA-CoA, 4-chlorobenzoyl-coenzyme A; 4-HBA, 4-hydroxybenzoate; 4-HBA-CoA, 4-hydroxybenzoyl-coenzyme A; 4-CBA-AMP, 4-chlorobenzoyl adenosine 5′-phosphate diester; K^+Hepes, *N*-(2-hydroxyethyl)piperazine-*N*′-2-ethanesulfonic acid, potassium salt; ATP, adenosine 5′-triphosphate; AMP, adenosine 5′-phosphate; NADH, dihydronicotinamide adenine dinucleotide; HPLC, high-performance liquid chromatography; Aad-Cys-D-Val, δ-(L-α-aminoadipyl)-L-cysteinyl-D-valine.

suggesting the presence of a CoA binding site on the enzyme and a possible role for the CoA in catalysis (*6*, *7*). Similarly, α-aminoadipate reductase activity is reportedly enhanced by reduced glutathione (*8*). Since most of the members of the superfamily are known to generate thioester intermediates or products (principally pantetheine or CoA adducts) from the acyl-adenylates they form, we shall henceforth refer to this group of enzymes as the "acyl-adenylate/thioester-forming" enzyme family. This family is structurally distinct from the acyladenylate forming aminoacyl-tRNA synthetase families (*9*) and the newly classified "N-type" ATP pyrophosphatase family (*10*).

The sequence identity existing between enzyme pairs from the acyl-adenylate/thioester-forming enzyme family is typically low (*ca.* 20−30%), which makes the generation of an accurate "unified alignment" of the sequences representing the different functions difficult if not impossible. Nonetheless, approximate alignments can be constructed, and from these, stretches of sequence that are highly conserved among all of the enzymes in this class can be identified (see, for example, refs *1*, *11*, and *12*). Illustrated in Figure 1, the most easily recognized of these is the **T**[SG]-**S**[G]-**G**-[ST]-**T**[SE]-**G**[S]-X-**P**[M]-**K**-**G**[LF] signature motif (the boldface letters represent residues that predominate at that position, with alternates given in brackets; X represents a hypervariable position), which we will refer to as motif I. A second highly conserved stretch of sequence is **Y**[LWF]-**G**[SMW]-X-**T**[A]-**E** (motif II, Figure 1). A third motif, **Y**[FL]-**R**[KX]-**T**[SV]-**G**-**D** (motif III, Figure 1) is conserved among all of the sequences representing this enzyme family except, oddly enough, the *Pseudomonas* sp. strain CBS3 4-CBA:CoA ligase sequence. The conservation of motifs I and II by all family members suggests that the two motifs may contribute to the ATP binding site, since ATP is the one substrate common to all members.

Recently, the first X-ray structure of a member of the adenylate/thioester-forming enzyme family, *Photinus pyralis* luciferase, was reported (*12*). Firefly luciferase has a unique fold consisting of a large N-terminal and small C-terminal domain. A majority of the invariant residues conserved in this family (*ca*. 7 total) are clustered on the surfaces of the domain−domain interface, suggesting this as the probable location of the catalytic site. The fact that the three sequence motifs represented in Figure 1 are also found here is consistent with the suggested role of these motifs in the binding/activation of the ATP substrate.

The present study was undertaken to examine the functions of motifs I and II in 4-CBA:CoA ligase, using site-directed mutagenesis to replace the stringently conserved residues indicated in boldface type: T-S-**G**-T-T-**G**-L-**P**-**K**-G (motif I) and Y-G-T-T-**E** (motif II). Steady-state and transient kinetic techniques were used to determine the impact of the amino acid replacements on catalysis of the adenylation and thioesterification steps of the overall reaction (Scheme 2) (*4*). In the text that follows, the results from these studies are presented and interpreted within the context of the luciferase structure as a means of examining structure−function relationships within the acyl-adenylate/thioester-forming enzyme family.

PROTEIN	***MOTIF I***	***MOTIF II***	***MOTIF III***
CoA Ligases:			
CBA.lig.P	**161TSGTTGLPKG170**	**302YGTTE306**	**376FRKAG380**
CBA.lig.A	**TSGTTGLPKA**	**YGTTE**	**YRTSD**
CBA.lig.Ar	**TSGTTGLPKG**	**YGTTE**	**YRTGD**
coum.lig.Ml	**TSGTTGPPKG**	**YGSTE**	**YRTGD**
coum.lig.Pc	**SSGTTGLPKG**	**YGMTE**	**LHTGD**
benz.lig.Rp	**SSGSTGRPKG**	**IGSTE**	**TKSGD**
osb.lig.S	**TSGTTGPQKA**	**FGMTE**	**FNTGD**
acet.Nc	**TSGSTGKPKG**	**YWQTE**	**YFTGD**
acyl.Po	**TSGTTGNPKG**	**WGMTE**	**FSTGD**
bile.lig.E	**SGGTSGKMKF**	**YSMTE**	**RSVGD**
Thiol-template Acyl-Adenylate Forming Enzymes:			
gram2.Bb	**1654TSGSTGKPKG1663**	**YGPTE**	**YRTGD**
tyr1.Bb	**178TSGTTGKPKG187**	**YGPTE**	**397YRTGD401**
EntE.Ec	**SGGTTGTPKL**	**FGMAE**	**YCSGD**
coron.lig.Ps	**TSGTTGITKG**	**YGTTE**	**IATGD**
enn.Fs	**TSGSTGKPKG**	**YGPTE**	**YRTGD**
angR.Va	**TSGSTGTPKG**	**GGATE**	**YRTGD**
Miscellaneous: Luciferase & α-Aminoadipate Reductase:			
luci.PHp	**198SSGSTGLPKG207**	**340YGLTE344**	**418LHSGD422**
luci.CbG	**SSGTTGLPKG**	**FGLTE**	**LHSGD**
ad.red.Sc	**TSGSEGIPKG**	**YGTTE**	**YRTGD**

FIGURE 1: Illustration of the sequence variation observed for the three motifs conserved throughout the acyl-adenylate/thioester enzyme superfamily. CBA.lig.P is 4-CBA:CoA ligase from *Pseudomonas* sp. strain CBS3 (*3*), CBA.lig.Al is 4-CBA:CoA ligase from *Alcaligenes* sp. strain AL3007 (*27*), CBA.lig.Ar is 4-CBA:CoA ligase from *Arthrobacter* sp. strain SU (*28*), coum.lig.Ml is coumarate:CoA ligase from *Mycobacterium leprae* (K. Robison, 1994, direct submission to Genbank, accession number 699196), coum.lig.Pc is coumarate:CoA ligase from *Petroselium crispinum* (*29*), benz.lig.Rp is 4-hydroxybenzoate:CoA ligase from *Rhodopseudomas palustris* (*30*), osb.lig.S is O-succinatebenzoyl:CoA ligase from *Staphylococcus aureus* (Tremblay and Sasarman, 1996: direct submission to Genbank, locus SAU51132, accession number U51132), acet.Nc is acetate:CoA ligase from *Neurospora crassa* (*31*), acyl.Po is acyl:CoA ligase from *Pseudomonas olevorans* (*32*), bile.lig.E is bile acid:CoA ligase from *Eubacterium* sp. strain VPI 12708 (*33*), tyr1.Bb is tyrocidine synthetase 1 from *Bacillus brevis*, gram2.Bb is gramicidin synthetase 2 from *Bacillus brevis*, (*34*), entE.Ec is enterobactin synthetase component E from *E. coli* (*35*), corn.lig.Ps is coronafacate ligase from *Pseudomonas syringae* (*36*), enn.Fs is enniatin synthetase from *Fusarium scripi* (*37*), angR.Va is anguibactin transacting transcriptional activator from *Vibrio anguillarum* (*38*), luci.PHp is luciferase from *Photinus pyralis* (*39*), luci.CbG is luciferase from the green-emitting strain of the click beetle (*40*), and ad.red.Sc is α-aminoadipate reductase from *Saccharomyces cerevisiae* (*41*).

MATERIALS AND METHODS

General. DNA digestions, gel electrophoreses, ligations, and transformations with competent *Escherichia coli* TG1 or JM101 cells were performed according to standard methods (*13*). Double-stranded DNA sequencing was accomplished using the USB DNA Sequenase kit (version 2) based on the dideoxy chain-termination method developed by Sanger et al. (*14*) and modified by Tabor and Richardson (*15*). Restriction enzymes and T4 DNA ligase with supplied buffers were purchased from New England Biolabs or USB. [7-^{14}C-4-CBA (21 mCi/mmol) and [α-^{35}S]dATP (1200 mCi/mmol) were purchased from CBN and NEN, respectively. The Geneclean II kit was purchased from BIO101 Inc. *E. coli* TG1 was obtained from Amersham. pUC18 and M13mp18 were purchased from USB and New England Biolabs, respectively. Primers for mutagenesis and sequencing were purchased either from Midland Certified Reagent Co. or from New England Biolabs. Reagents, buffers, and the protein concentration assay kit [based on the Lowry method (*16*)] were obtained from Sigma. PCR reactions were carried out on a Thermolyne Model Temp•Tronic thermocycler, DNA sequencing on a BRL Model L2 electrophoresis unit, and enzyme activity assays were on a

Gilford spectrophotometer, Model 250. Rapid quench experiments were performed on a KinTek quench flow apparatus (three-syringe model equipped with a thermostatically controlled circulator), SDS−PAGE analyses on a BRL Model V-16 vertical slab gel unit using the method of Laemmli (*17*) and HPLC analysis on a Beckman Model 110A HPLC system equipped with a Hitachi Model 100-10 spectrophotometer. Liquid scintillation counting was carried out with a Beckman Model LS 5801 counter and circular dichroism spectra were measured with a Jasco J-500C spectropolarimeter.

Construction of the K169M Mutant. The *Sac*I−*Sph*I DNA fragment (2050 bp) was cut from the *Nru*I−*Nhe*I pUC18 subclone (*18*) and ligated into the polylinker region of M13mp18 RF. The recombinant vector was used to transform competent *E. coli* TG1 cells. The single-strand DNA of the recombinant M13mp18 RF was prepared according to standard methods (*13*) and used as a template for mutagenesis. The primer used, 5′-CACCGCTCCCA-TGGGCAAACC-3′, anneals to the plus strand region corresponding to residues 172−166 of the ligase. The mutagenesis (*19*) was carried out using Amersham oligonucleotide-directed mutagenesis kit 2.1 according to the manufacturer's instruction. The mutated *Sac*I−*Sph*I DNA fragment was removed and reinserted in the polyclonal region of pUC18. The hybrid vector was used to transform competent *E. coli* JM101 cells. The sequence of the mutant was verified by DNA sequencing.

Construction of the G163I, G166I, P168A, and E306Q Mutants. The *Nru*I−*Nhe*I pUC18 recombinant plasmid was used as template for mutagenesis using the PCR method. M13(-47) universal and M13(-48) reverse primers were used as the outside primers. The inside primers used are 5′-TACACGTCGATCACAACCGGTTTG-3′ and 5′-ACCG-GTTGTGATCGACGTGTAGAA-3′ for G163I; 5′-GGGA-CAACCATTTTGCCCAAGGGA-3′ and 5′-CTTGGGC-AAAATGGTTGTCCCCGA-3′ for G166I; 5′-ACCGGTTTG-GCCAAGAAGGGAGCG-3′ and 5′-TCCCTTGGCCAAAC-CGGTTGT-3′ for P168A; 5′-GGAACAACACAAGCGAT-GAAT-3′ and 5′-CATCGCTTGTGTTGTTCCGTA-3′ for E306Q. The mutagenesis reaction was carried out using the Perkin-Elmer Cetus GeneAmp PCR kit. A 0.5 mL thin-walled GeneAmp microfuge tube was used to contain a 100 μL reaction mixture consisting of 2.5 mM $MgCl_2$, 200 μM each dATP, dGTP, dCTP, and dTTP, 25 pmol of each primer, $(1 \times 10^8) - (1 \times 10^9)$ molecules of DNA template, and 2.5 units of *Taq* DNA polymerase in the supplied buffer. The reaction was overlaid with 50 μL of sterile silica oil. A typical reaction period included 5 min at 94 °C for denaturation and 5 min at the annealing temperature, followed by 25 cycles of 1.5 min at 72 °C for extension, 1 min at 92 °C for denaturation, and 1 min at the annealing temperature with a final extension of 10 min at 72 °C. The PCR products were isolated by agarose gel electrophoresis and purified using Geneclean II. The secondary PCR reaction was carried out with 1 μg of PCR product using a reaction program consisting of 5 min at 94 °C and 5 min at annealing temperature, followed by 5 cycles of 1.5 min at 72 °C, 1 min at 92 °C, and 1 min at the annealing temperature. After 5 cycles, the reaction was brought to 25 °C and 25 pmol of each pair of external primers was added. The reaction period then consisted of 5 min at 94 °C and 5 min at the annealing temperature, followed by 25 cycles of 1.5 min at 72 °C, 1 min at 92 °C, and 1 min at the annealing temperature with final extension of 10 min at 72 °C. The PCR products were purified and then digested with *Sac*I and *Sph*I. The *Sac*I−*Sph*I fragment was inserted into the polylinker site of pUC18 and the recombinant plasmid was used to transform competent *E. coli* JM101 cells. The sequence of the mutant was verified by DNA sequencing.

Purification of the 4-CBA:CoA Ligase Mutants. The K169M mutant protein was purified by employing the same procedure (0−50% ammonium sulfate fractionation followed by DEAE ion-exchange chromatography) used for purification of the wild-type ligase (*18*). The G163I, G166I, P168A, and E306Q mutants were purified by using, in addition to 0−50% ammonium sulfate fractionation and DEAE-cellulose column chromatography, Sephadex G-100 column chromatography (1.5 × 90 cm; 50 mM K^+Hepes, pH 7.5 containing 0.1 N NaCl as elution buffer). The mutant proteins were detected by measuring ligase activity using the spectrophotometric coupled assay (see below) and/or by examining SDS−PAGE mobility.

K_m and k_{cat} Measurement. 4-CBA-CoA formation was monitored at 340 nm ($\Delta\epsilon = 6.2$ $mM^{-1}cm^{-1}$) as NADH is oxidized in the coupled assay consisting of myokinase, pyruvate kinase, and lactate dehydrogenase. One milliiter reaction solutions contained 0.2 mM NADH, 3 mM PEP, 10 mM $MgCl_2$, 5 mM KCl, 11 units of myokinase, 9 units of pyruvate kinase, and 9 units of lactate dehydrogenase in 50 mM K^+Hepes (pH 7.5, 25 °C).The ligase concentrations used are 0.035 μM wild-type, 2 μM G163I, 0.3 μM G166I, 0.05 μM K169M, and 1.4 μM E306Q. The first set of initial velocity measurements were made using varying 4-CBA concentration (5 μM−2 mM) and fixed ATP (8 mM) and CoA (1 mM) concentrations. For the second set of measurements the CoA concentration was varied (0.02−2 mM) at fixed 4-CBA (2 mM) and ATP (8 mM) concentrations. Finally, the ATP concentration was varied (0.15−9 mM) at fixed 4-CBA (2 mM) and CoA (1 mM) concentrations. The K_m and V_{max} data were calculated from the initial velocity data using eq 1 and the Fortran HYPERL program (*20*):

$$v_o = V_{max}[E][S]/K_m + [S] \quad (1)$$

where v_0 = initial velocity, V_{max} = maximum velocity, [E] = total enzyme concentration, [S] = substrate concentration, and K_m = Michaelis constant for substrate. The k_{cat} was calculated by dividing the V_{max} value by the concentration of ligase present in the reaction mixture.

Single-Turnover (Partial) Reactions of 4-CBA + MgATP. All reactions were performed at 25 °C using a rapid quench instrument (except in the case of the G163I mutant). Each reaction was initiated by mixing 43 μL of 60 μM of the enzyme solution in 50 mM K^+Hepes (pH 7.5) with 43 μL of the solution containing 16 μM [^{14}C]-4-CBA (0.01 μCi), 16 mM ATP, and 20 mM $MgCl_2$ in 50 mM K^+Hepes (pH 7.5). The final concentrations after mixing (in a total volume of 86 μL) were 30 μM enzyme, 8 μM [^{14}C]-4-CBA (0.01 μCi), 8 mM ATP, and 10 mM $MgCl_2$. After incubation for a specified period of time, the reaction mixture was quenched by the addition of 164 μL of 0.1 M HCl. The quenched solution was collected in a 1 mL syringe and then transferred to a 1.5 mL Eppendorf tube containing 100 μL of CCl_4. Following vigorous vortexing, the precipitated protein was pelleted by centrifugation for 2 min at 14 000 rpm in a

microfuge. The supernatant (250 μL) was stored at −80 °C (for ∼24 h) until HPLC analysis was performed. The 4-CBA and 4-CBA-AMP present in the reaction mixture were separated on a C-18 reversed-phase column (Beckman Ultrasphere; 4.6 × 25 cm) at a flow rate of 1 mL/min using added unlabeled 4-CBA and 4-CBA-AMP (prepared as described in (ref *4*) to locate peak positions. The elution program used was 100% solvent A (25% methanol, 2.5% triethylamine, and 25 mM K^+P_i adjusted to pH 6.5 with H_3PO_4) for 2 min, 0−100% solvent B (50% methanol, 2.5% triethylamine, and 25 mM K^+P_i adjusted to pH 6.5 with H_3PO_4), and then 100% solvent B for 5 min. The AMP and eluted at the solvent front (3−4 min) while 4-CBA eluted at 19 min and 4-CBA-AMP at 22 min. The 4-CBA and 4-CBA-AMP were quantitated by measuring the ^{14}C radioactivity of the HPLC effluent corresponding to the peak positions using scintillation counting techniques.

Single-Turnover Reactions of 4-CBA + MgATP + CoA. All reactions were performed at 25 °C in a rapid quench instrument (except in the case of the G163I mutant). Each reaction was initiated by mixing 43 μL of 60 μM of the enzyme solution in 50 mM K^+Hepes (pH 7.5) with 43 μL of the solution containing 16 μM [^{14}C] 4-CBA (0.01 μCi), 16 mM ATP, 20 mM $MgCl_2$, and 2 mM CoA in 50 mM K^+Hepes (pH 7.5). The final concentrations after mixing (86 μL) were 30 μM enzyme, 8 μM [^{14}C]-4-CBA (0.01 μCi), 8 mM ATP, 10 mM $MgCl_2$, and 1 mM CoA. After incubation for a specified period of time, the reaction was quenched with acid and treated in the same way as described above. The protein-free solution was kept at −80 °C (for ∼24 h) until HPLC analysis was performed as described in the previous section. The 4-CBA, 4-CBA-AMP, and 4-CBA-CoA (retention time 33 min) were quantitated by measuring the ^{14}C radioactivity of the HPLC effluent corresponding to the peak positions using scintillation counting techniques.

Transient Kinetic Data Analysis. The apparent first-order rate constants observed for the ligase-catalyzed single turnover reactions were determined by computer fitting the data (input reaction time versus concentration as *x*, *y* pairs) obtained from the rapid quench experiments to the first-order rate equations shown in eqs 2 and 3 using the KaleidaGraph nonlinear regression computer program:

$$[S]_t = [S]_{max} - [P]_{max}(1 - e^{-kt}) \quad (2)$$

$$[P]_t = [P]_{max}(1 - e^{-kt}) \quad (3)$$

Determination of the first-order rate constants for the forward and reverse reactions was carried out by iterative curve fitting to the rate profiles with the computer simulation program KINSIM as described in ref *4*.

Determination of 4-CBA Binding Constant by Fluorescence Titration. Equilibrium fluorescence measurements were made at 25 °C using a Spex Fluorolog instrument equipped with two 1681 0.22 m spectrometers interfaced with a Tantung 386 computer (using dM 3000 software). The excitation wavelength was 280 nm (4-CBA does not absorb beyond 260 nm) and the spectra were recorded in the range of 300−450 nm for 3 mL solutions containing 0.9−1.0 μM ligase and 0−180 μM 4-CBA (added in 1 μL aliquots) in 50 mM K^+Hepes, pH 7.5. For the titration experiments the observed fluorescence at 350 nm was plotted vs [4-CBA] and the curve analyzed with eq 4 using the KaleidaGraph nonlinear regression computer program:

$$\Delta F_{obs} = \Delta F_{max}/(1 + K_d/[S]) \quad (4)$$

where K_d = 4-CBA dissociation constant, ΔF_{obs} = observed change in fluorescence, ΔF_{max} = total change in fluorescence, and [S] = 4-CBA concentration (*21*).

Table 1: Steady-State Kinetic Constants of Wild-Type and Mutant 4-CBA:CoA Ligase[a]

	4-CBA[a]	ATP[b]	CoA[d]
		K_m (μM)	
WT	14 ± 2	308 ± 14	85 ± 4
G163I	105 ± 11	1314 ± 90	62 ± 15
G166I	73 ± 6	981 ± 84	108 ± 14
P168A[e]	ND	ND	ND
K169M	20 ± 1	830 ± 81	76 ± 4
E306Q	253 ± 43	321 ± 47	168 ± 23
		k_{cat} (s^{-1})	
WT	34 ± 2	54 ± 2	39 ± 1
G163I	0.036 ± 0.002	0.039 ± 0.002	0.04 ± 0.005
G166I	2.3 ± 0.1	3.3 ± 0.6	2.7 ± 0.2
P168A[e]	ND	ND	ND
K169M	9.8 ± 0.2	16 ± 1	9.4 ± 0.2
E306Q	0.7 ± 0.06	0.9 ± 0.04	0.8 ± 0.06

[a] Determined in 50 mM K^+Hepes and 1 mM DTT at pH 7.5 and 25 °C. [b] Measured in the presence of 3.5 mM ATP, 5 mM Mg^{2+}, and 1 mM CoA for the wild-type enzyme or 8 mM ATP, 10 mM Mg^{2+}, and 1 mM CoA for the mutants. [c] Measured in the presence of 2 mM 4-CBA, 5 mM Mg^{2+}, and 1 mM CoA for the wild-type enzyme or 2 mM 4-CBA, 10 mM Mg^{2+}, and 1 mM CoA for the mutants. [d] Measured in the presence of 2 mM 4-CBA, 5 mM Mg^{2+}, and 1 mM CoA for the wild-type enzyme or 2 mM 4-CBA, 8 mM ATP, and 10 mM Mg^{2+} for the mutants. [e] Not determined because the activity of the P168A mutant was too low to be measured using the initial velocity techniques.

RESULTS

Construction, Purification, and Characterization of Mutant 4-CBA:CoA Ligases. The K169M mutant was constructed using the phosphorothiolate method (*19*) and the G163I, G166I, P168A, and E306Q mutants were constructed using the PCR method (*22*). All mutants were expressed in the same cell line used to express the wild-type gene: *E. coli* JM101. The K169M mutant ligase was purified using the same ammonium sulfate fractionation and DEAE-cellulose chromatography steps used to purify wild-type ligase (*18*), whereas the other mutants required an additional purification step consisting of Sephadex G-100 column chromatography. The yields of the purified enzymes obtained (per 1 g of cell paste) are 2 mg of wild-type, 2 mg of K169M, 0.2 mg of G163I, 0.2 mg of G166I, 0.1 mg of E306Q and 0.05 mg of P168A ligase. Circular dichroism spectra were measured for wild-type, K169M, G163I, and G166I ligases (1 μM ligase in 5 mM KH_2PO_4/1 mM DTT, pH 7.5 at 25 °C) and found to be essentially identical: trough λ_{max} at 220 nm, $\theta = -12 \times 10^6$ deg·cm^2/dmol.

Steady-State Kinetic Constants of Wild-Type and Mutant 4-CBA:CoA Ligases. The k_{cat} and K_m values were determined at pH 7.5, 25 °C, by carrying out initial velocity experiments in which the Mg(II) activator and two of the substrates were held at a fixed, saturating concentration while the third was varied in the range of (0.5−10)K_m. The results obtained are shown in Table 1. We were unable to detect catalytic activity in the P168A mutant using the spectrophotometric coupled assay.

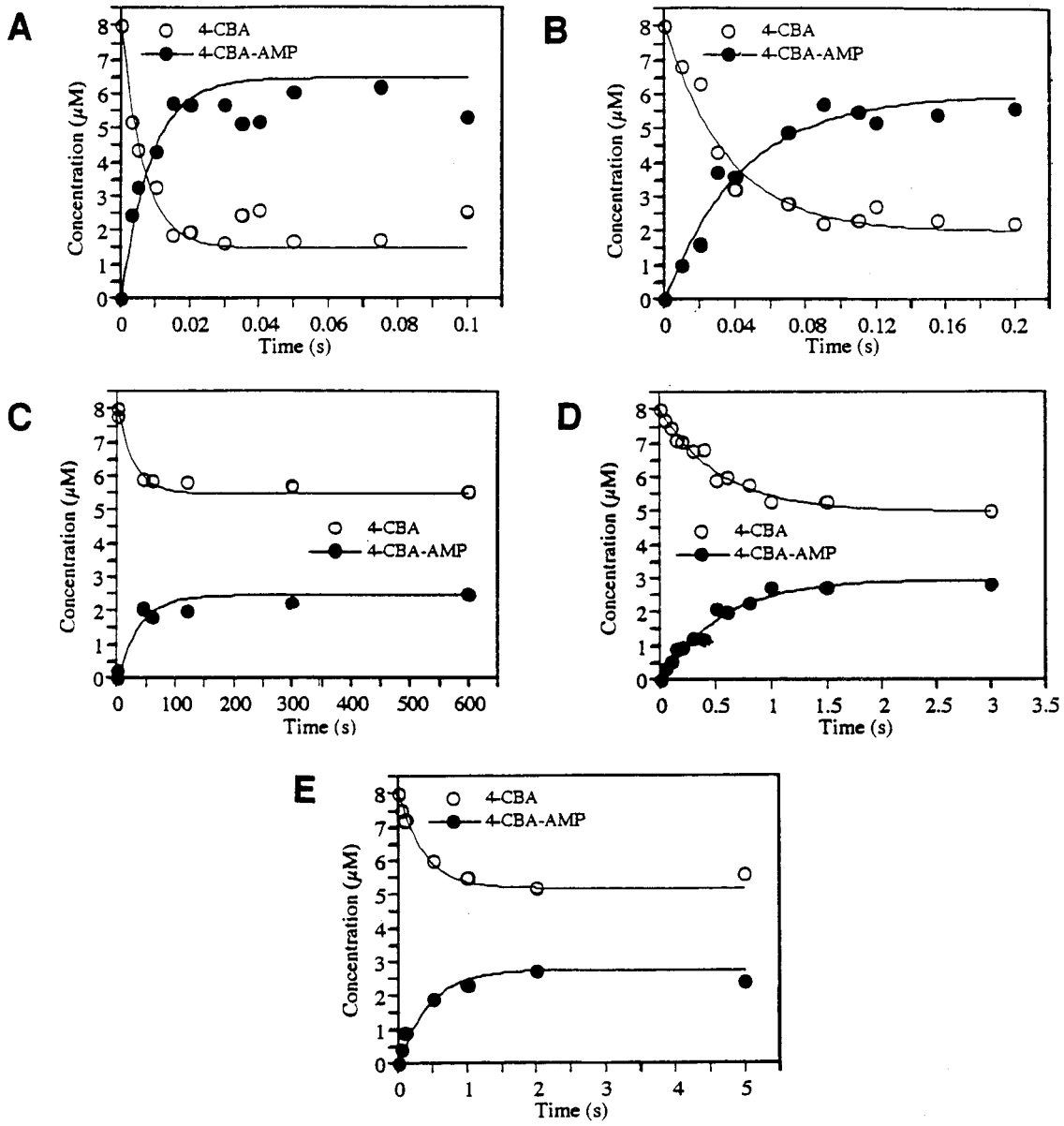

FIGURE 2: Time course for a single turnover of 4-CBA + MgATP catalyzed by 4-CBA:CoA ligase at 25 °C in 50 mM K^+Hepes (pH 7.5). The final concentrations of reactants in the 86 μL reaction mixture were 8 μM 4-CBA, 8 mM ATP, and 5 mM $MgCl_2$ and 30 μM (A) wild-type, (B) K169M mutant, (C) G163I mutant, (D) G166I mutant, or (E) E306Q mutant ligase. After various reaction periods (milliseconds), the solution was quenched with 164 μL of 0.1 N HCl. The 4-CBA and 4-CBA-AMP present in the reaction mixtures were analyzed by HPLC as described in Materials and Methods. The curves shown in the figure were generated using eqs 2 and 3 and the KaleidaGraph nonlinear regression computer program.

Single-Turnover Profiles for the Partial Reaction 4-CBA + ATP → 4-CBA-AMP + PP_i Catalyzed by Wild-Type and Mutant Ligases. The profiles for single-turnover reactions of 4-CBA and ATP in the active sites of wild-type and mutant 4-CBA:CoA ligases were measured by reacting radiolabeled 4-CBA (8 μM) with excess ligase (30 μM) in the presence of saturating ATP and Mg(II). The reactions were quenched at varying conversion with acid, and the 4-CBA and 4-CBA-AMP released from the enzyme were separated by HPLC and quantitated by liquid scintillation counting. The profiles for wild-type, K169M, G163I, G166I, and E306Q ligases are shown in Figure 2 (the P168A mutant was inactive). The ratios of the 4-CBA-AMP to 4-CBA observed at the completion of the single-turnover reactions are listed in Table 2. These ratios serve as rough estimates of the internal equilibrium constants = [E·4-CBA-AMP·PP_i]/[E·4-CBA·ATP].[2] The 4-CBA decay curves and 4-CBA-AMP formation curves were analyzed using eqs 2 and 3 to obtain apparent first-order rate constants. These are listed as app k_1 in Table 2. In previous studies of the wild-type ligase (*4*) we showed that under the reaction conditions employed in the single-turnover experiments substrate binding is not rate-limiting. Thus, the apparent first-order rate constants derived from the rate data shown in Figure 2A

[2] This ratio will deviate from the true internal equilibrium constant to the extent that 4-CBA and 4-CBA-AMP partition off the enzyme into solution. At 8 μM 4-CBA (K_d = 5 μM; Figure 4) and 30 μM ligase, we calculate that 83% of the 4-CBA will be enzyme-bound. While we do not yet know the K_d of the 4-CBA-AMP and PP_i, our expectation is that the former remains tightly bound to the wild-type enzyme in order to maximize the efficiency of the ensuing reaction with CoA. We also note that the K_d for 4-CBA is the same for wild-type and mutant ligases (K169M, G163I) and that the ATP was saturating in the reaction mixture. Thus, the reduction observed in the ratio of 4-CBA-AMP to 4-CBA observed for the mutant ligases may reflect a shift in the relative stability of enzyme−substrate vs enzyme intermediate complexes.

Table 2: Rate Constants for the Adenylation Partial Reaction and for the Adenylation and Thioesterification Steps of the Full Reaction Catalyzed by Wild-Type and Mutant 4-CBA:CoA Ligases

	E·4-CBA·ATP → E·4-CBA-AMP·PP_i[a]				E·4-CBA·ATP·CoA → E·4-CBA-AMP·PP_i·CoA → E·4-CBA-CoA·AMP·PP_i[b]					
ligase	app k_1 (s^{-1})	app K_1[c]	k_1 (s^{-1})	k_{-1} (s^{-1})	app k_1[d] (s^{-1})	app k_2[e] (s^{-1})	k_1 (s^{-1})	k_{-1} (s^{-1})	k_2 (s^{-1})	k_{-2} (s^{-1})
wild type	136 ± 13[f] 120 ± 20[g]	4	135	5	99 ± 4	73 ± 8	135	35	100	10
K169M	28 ± 3[f] 23 ± 2[g]	3	25	8	24 ± 1	18 ± 1	25	8	100	10
G166I	1.9 ± 0.1[f] 1.9 ± 0.1[g]	0.6	1.5	3	1.9 ± 0.1	1.6 ± 0.1				
G163I	0.036 ± 0.005[f] 0.027 ± 0.006[g]	0.3	0.04	0.1	0.037 ± 0.005	0.036 ± 0.007				
E306Q	2.7 ± 0.4[f] 2.3 ± 0.4[g]	0.5	2.5	5	2.2 ± 0.2	1.9 ± 0.3				

[a] Reactions contained 30 μM ligase, 8 μM [^{14}C]-4-CBA, 8 mM ATP, and 10 mM $MgCl_2$ in 50 mM K^+Hepes (pH 7.5, 25 °C). See Figure 2. [b] Reactions contained 30 μM ligase, 8 μM [^{14}C]-4-CBA, 8 mM ATP, 1 mM CoA, and 10 mM $MgCl_2$ in 50 mM K^+Hepes (pH 7.5, 25 °C). See Figure 3. [c] Apparent internal equilibrium constant = [E·4-CBA-AMP·PP_i]/[E·4-CBA·ATP] determined from the ratio of 4-CBA and 4-CBA-AMP at equilibrium in Figure 2. [d] Rate constant derived from first order fit of 4-CBA decay curve in Figure 3. [e] Rate constant derived from first order fit of 4-CBA-CoA formation curve in Figure 3. [f] Rate constant derived from first order fit of 4-CBA decay curve in Figure 2. [g] Rate constant derived from first order fit of 4-CBA-AMP formation curve in Figure 2.

reflect the sum of the forward and reverse rate constants (k_1 and k_{-1}) for the equilibration of E·4-CBA·ATP and E·4-CBA-AMP·PP_i. We assume that the same holds true for the single-turnover reactions of the mutant ligases. The forward (k_1) and reverse (k_{-1}) rate constants were defined by an iterative process using the simulation program KINSIM and the estimates of the rate constants to simulate 4-CBA decay and 4-CBA-AMP formation curves (see Table 2). Comparisons of the app k_1 or the simulated k_1 and k_{-1} values leads to the conclusion that the amino acid replacement at K169, G166, G163, or E306 significantly inhibits the adenylation partial reaction.

Single-Turnover Profiles for the Reaction 4-CBA + ATP + CoA → 4-CBA-CoA + AMP + PP_i Catalyzed by Wild-Type and Mutant Ligases. The profiles for a single-turnover reaction of 4-CBA, ATP, and CoA in the active sites of wild-type and mutant 4-CBA:CoA ligases were measured by reacting radiolabeled 4-CBA (8 μM) with excess ligase (30 μM) in the presence of saturating ATP, CoA, and Mg(II). The reactions were quenched at varying conversion with acid, and the 4-CBA, 4-CBA-AMP, and 4-CBA-CoA released from the enzyme were separated by HPLC and quantitated by liquid scintillation counting. The profiles obtained for wild-type, K169M, G163I, G166I, and E306Q ligases are shown in Figure 3. The 4-CBA decay curves were analyzed using eq 2 to determine the apparent rate constants (app k_1, see Table 2) for the adenylation partial reactions, and the 4-CBA-CoA formation curves were analyzed using eq 3 to determine the apparent rate constants (app k_2) for the thioesterification partial reaction.

The accumulation of 4-CBA-AMP intermediate in the active site of the wild-type ligase reaches 25% of the 4-CBA reactant (Figure 3A). For the K169M ligase, the 4-CBA-AMP accumulates to a maximum of 6% (Figure 3B) while for the G166I, G163I, and E306Q ligases the intermediate does not accumulate to a noticeable extent (Figure 3C−E). In a previous paper (*4*) we had reported the use of the simulation program KINSIM to define $k_1 = 135\ s^{-1}$, $k_{-1} = 35\ s^{-1}$, $k_2 = 100\ s^{-1}$ and $k_{-2} = 10\ s^{-1}$ by iterative curve fitting to the single turnover profiles of Figure 2A and Figure 3A. The same operation carried out on the K169M ligase profiles (Figures 2B and 3B) generates the rate constants $k_1 = 25\ s^{-1}$, $k_{-1} = 8\ s^{-1}$, $k_2 = 100\ s^{-1}$, and $k_{-2} = 10\ s^{-1}$. Comparison of these two sets of rate constants leads to the conclusion that the K169M mutation inhibits the adenylation partial reaction but not the thioesterification reaction. For the G166I, G163I, and E306Q mutants only the app k_1 and app k_2 values of Table 2 are available for comparison (the simulations of the individual rate constants require a 4-CBA-AMP curve for fitting and these mutants do not yield one). Nevertheless, it is clear that the adenylation reaction is inhibited in these mutants.

Determination of the 4-CBA Binding Constant by Fluorescence Titration. The fluorescence spectra of 1 μM wild-type 4-CBA:CoA ligase measured in the absence and presence of saturating 4-CBA are shown in Figure 4 along with the fluorescence titration curve determined at 350 nm. The fluorescence spectra and titration curves obtained with the K169M and G163I mutants (not shown) closely resemble those of the wild-type ligase. With each ligase, bound 4-CBA quenches *ca.* 25% of the intrinsic fluorescence. The titration curves were analyzed using equation 4 to give the following K_d values: 4.9 ± 0.2 μM for wild-type, 5.1 ± 0.4 μM for K169M, and 3.6 ± 0.6 μM for G163I 4-CBA:CoA ligase.

DISCUSSION

Interpretation of the Kinetic Properties of the 4-CBA:CoA Ligase Site Directed Mutants in Terms of Catalysis of the Adenylation−Thioesterification Partial Reactions. The steady-state kinetic analysis of the wild-type and mutant ligases revealed that the turnover rate, which is 40 s^{-1} in wild type, is reduced 4-fold in the K169M mutant, 14-fold in the G166I mutant, 50-fold in the E306Q mutant, 1000-fold in the G163I mutant, and greater than 5000-fold in the P168A mutant (Table 1). The G163, G166, P168, and K169 residues of motif I (TS**G**ST**G**L**PK**G) and the E306 residue of motif II (YGTT**E**) (Figure 1) were thus shown to be important for catalysis of the overall reaction.

The overall 4-CBA:CoA ligase reaction consists of an adenylation step (which can take place in the absence of the CoA substrate) followed by a thioesterification step (Scheme 2). The transient kinetics of these two steps had been examined in a previous study of the wild-type ligase using rapid quench techniques in conjunction with radiolabeled substrate. Here the forward rate constant for the adenylation

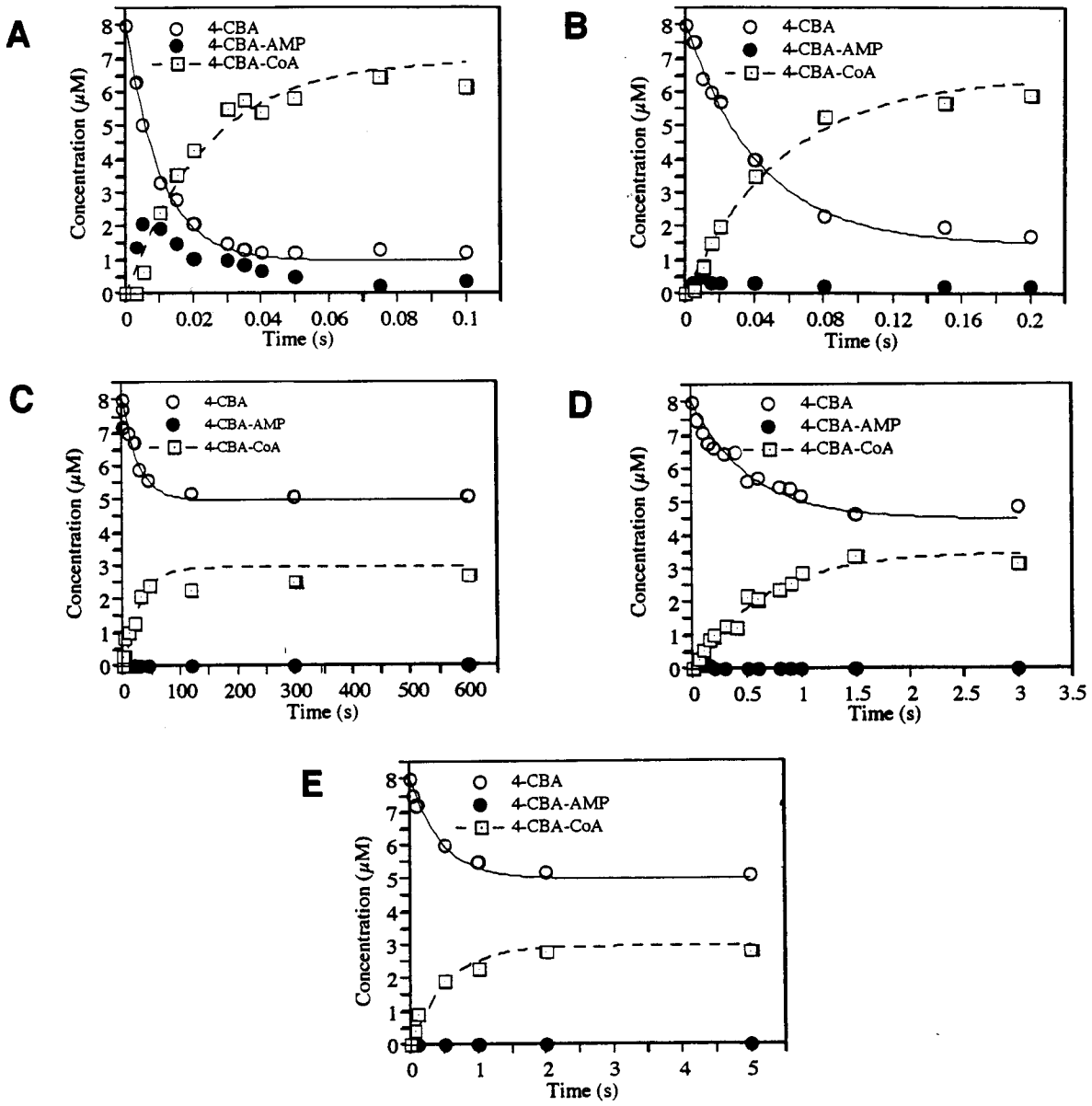

FIGURE 3: Time course for a single turnover of 4-CBA + MgATP + CoA catalyzed by 4-CBA:CoA ligase at 25 °C in 50 mM K^+Hepes (pH 7.5). The final concentrations of reactants in the 86 μL reaction mixture were 8 μM 4-CBA, 8 mM ATP, and 5 mM $MgCl_2$ and 30 μM (A) wild-type, (B) K169M mutant, (C) G163I mutant, (D) G166I mutant, or (E) E306Q mutant ligase. After various reaction periods (milliseconds), the solution was quenched with 164 μL of 0.1 N HCl. The 4-CBA, 4-CBA-AMP, and 4-CBA-CoA present in the reaction mixtures were analyzed by HPLC as described in Materials and Methods. The curves shown in the figure were generated using eqs 2 and 3 and the KaleidaGraph nonlinear regression computer program.

step of the full reaction was determined as 135 s^{-1}, and that for the thioesterification step, 100 s^{-1} (*4*). Transient kinetic studies of the adenylation and thioesterification steps catalyzed by the ligase mutants were carried out in the present study to see which of these two steps had been inhibited by the amino acid replacement made in the mutant enzyme.

Catalysis of the adenylation partial reaction by the ligase mutants was accessed in single-turnover experiments where excess ligase was reacted with radiolabeled 4-CBA in the presence of saturating MgATP and absence of CoA. The single-turnover time courses measured for the ligase mutants (Figure 2) differ from that measured for wild-type ligase in two respects. First, the ratio of the 4-CBA-AMP to 4-CBA observed at the completion of the single turnover reaction is reduced (from 4 for the wild-type ligase down to 0.3 for the G163I ligase mutant; Table 2). This reduction may reflect a decreased internal equilibrium constant = [E·4-CBA-AMP·PP_i]/[E·4-CBA·ATP] and hence a decreased ability to stabilize the acyl-adenylate intermediate in the mutant enzyme. Second, the rate constants for the 4-CBA-AMP formation are reduced (roughly 5-fold in the K169M mutant, 60-fold in the G166I mutant, 50-fold in the E306Q mutant, and 4000-fold in the G163I mutant; Table 2). This pattern is very similar to the pattern observed in k_{cat} values (Table 1) determined from the multiple-turnover (steady-state initial velocity) experiments and is a clear indication that the mutations made at motifs I and II inhibit the adenylation step.

Catalysis of the thioesterification partial reaction was examined in single- turnover experiments where excess enzyme was reacted with radiolabeled 4-CBA in the presence of saturating MgATP and CoA (Figure 3). In the case of the wild-type enzyme, the rate of disappearance of 4-CBA slightly exceeds the rate of appearance of 4-CBA-CoA and the transient accumulation of the 4-CBA-AMP intermediate is clearly evident (to a maximum level of 25%) (Table 2).

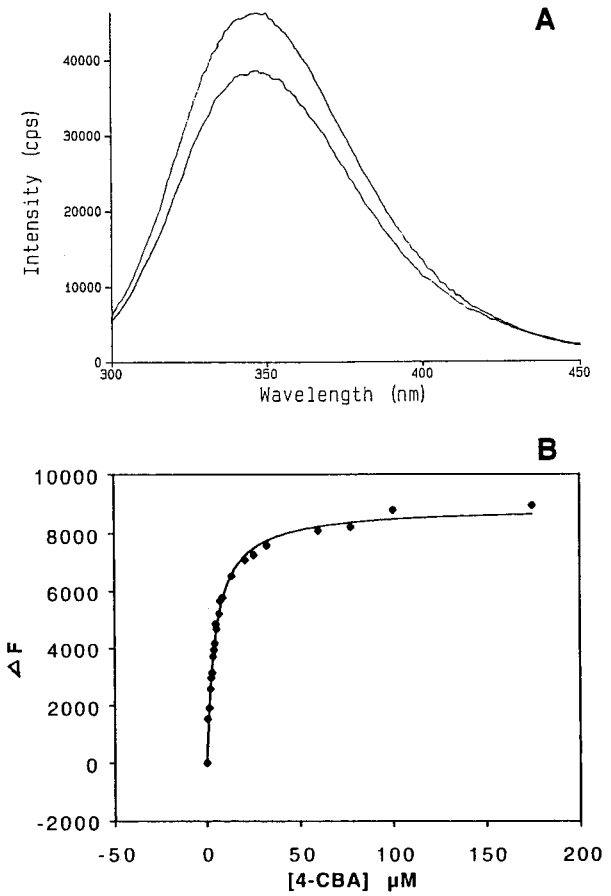

FIGURE 4: (A) *Top curve*, equilibrium fluoresence spectrum of 1 μM wild-type 4-CBA:CoA ligase in 50 mM K^+Hepes, pH 7.5 at 25 °C, using an excitation wavelength of 280 nm. *Bottom curve*, same spectrum measured in the presence of 13 μM 4-CBA (4-CBA does not absorb beyond 260 nm). (B) Titration of 1 μM wild-type 4-CBA:CoA ligase in 50 mM K^+Hepes, pH 7.5 at 25 °C with 4-CBA. The observed fluoresence at 350 nm is plotted vs [4-CBA]. The curve was analyzed using eq 4 and the KaleidaGraph nonlinear regression computer program.

In the case of the mutant ligases the rate of disappearance of 4-CBA during the single turnover is reduced and there is a corresponding reduction in the rate of appearance of 4-CBA-CoA (Figure 3; Table 2). Furthermore, only the K169M mutant showed significant accumulation of the 4-CBA-AMP intermediate and here the level was reduced from 25% for wild-type to 6% for the mutant in parallel with the 4-fold decrease observed in the rate of 4-CBA disappearance (Figure 3). These results suggest that the adenylation step has become rate-limiting in these mutants. From the steady-state kinetic data (Table 1) we find that the K_m measured for CoA with these mutants is unchanged while those for 4-CBA and ATP are significantly increased. This finding is consistent with the view that it is the adenylation partial reaction and perhaps not the thioesterification partial reaction that is inhibited by the amino acid replacements made at motifs I and II.

Comparison of the Kinetic Properties of the 4-CBA:CoA Ligase Site Directed Mutants with Those of Tyrocidine Synthetase 1 and Gramicidin Synthetase 2 Mutants. Although the acyl-adenylate/thioester-forming enzyme family contains many members, mutants involving motifs I−III (Figure 1) have been reported (to the best of our knowledge) only in the case of tyrocidine synthetase 1 (TycA) and gramicidin synthetase 2 (see Scheme 2) (*23*, *24*). The amino acid substrates of these enzymes are activated for thiol-template peptide bond formation by adenylation with ATP. The substitution of the first glycine of motif I in gramicidin synthetase 2 (G1656) with aspartate shut down the ATP−PP_i exchange activity of the valine activating domain (*23*). In the case of 4-CBA:CoA ligase where the first and second glycine residues of motif I (G163 and G166) were separately replaced with isoleucine residues, catalytic activity was also significantly inhibited. In contrast, the conservative replacement of G180, G183, and G187 of motif I in TycA with alanine did not inhibit the exchange activity (*24*).

In the case of the K169M 4-CBA:CoA ligase mutant, substitution of the highly conserved lysine residue of motif I resulted in a 4-fold drop in catalytic activity. Replacement of this residue (K186) in TycA with arginine or threonine resulted in a 10- or 50-fold drop in activity, respectively. The fact that these mutants are only partially inhibited in function suggests that the lysine residue does not assume a major role in ATP binding or in transition state stabilization. Thus, the role of the Lys residue of motif I must be quite different than that of the essential Lys residue of the P-loop motif (GXXGXGKT/S or GXXXXGK) found in many ATP-phosphotransferases (*25*, *26*).

Motif III, which is highly conserved in all of the sequences representing the acyl-adenylate/thioester forming enzyme family (except for the *Pseudomonas* sp. strain CBS3 4-CBA:CoA ligase sequence) (Figure 1) contains the stringently conserved aspartate residue. Interestingly, replacement of this aspartate (D401) in TycA with asparagine did not significantly inhibit the exchange reaction and substitution with serine resulted in only a 10-fold decrease in the exchange rate. Conservation of the aspartate may be driven by a supportive structural role (see below) rather than an essential catalytic role.

Interpretation of the Kinetic Properties of the 4-CBA:CoA Ligase Mutants within the Framework of the Firefly Luciferase Crystal Structure. Of the members of the acyl-adenylate/thioester-forming enzyme family, only luciferase from firefly has been structurally characterized. The crystal structure of firefly luciferase (illustrated in Figure 5) defines a new fold, which may be assumed to be representative of the folds associated with the entire acyl-adenylate/thioester-forming enzyme family, including the 4-CBA:CoA ligase (*12*). The N-terminal domain comprises the major portion of the luciferase structure (residues 4−436) and consists of a distorted antiparallel β-barrel and two β-sheets, which are flanked on either side by α-helices (Figure 5A). A wide cleft, presumed to be the active site, separates the N-terminal domain from the smaller ($\alpha+\beta$)-C-terminal domain (residues 440−544). In Figure 5A, motif I (198SSGSTGLPKG207) is represented in blue, motif II (340YGLTE344) in red, and motif III (418LHSGD422) in green. All three motifs form loops on the N-terminal which line one side of the cleft separating the two domains. The blue loop of motif I, truncated, is shown using only residues S198, L204, P205, and K206 since the structure of the region 199SGSTG203 is disordered in the crystal. Nevertheless, we can see in Figure 5B a possible H-bonding interaction between the Ser198 of motif I and the invariant residue Glu344 of motif II. Motif II in turn interacts with motif III through an H-bond formed between the hydroxyl group of Tyr340 and the carboxyl group of the highly conserved Asp422 (Figure 5B). It is clear from this structure that the regions of conserved

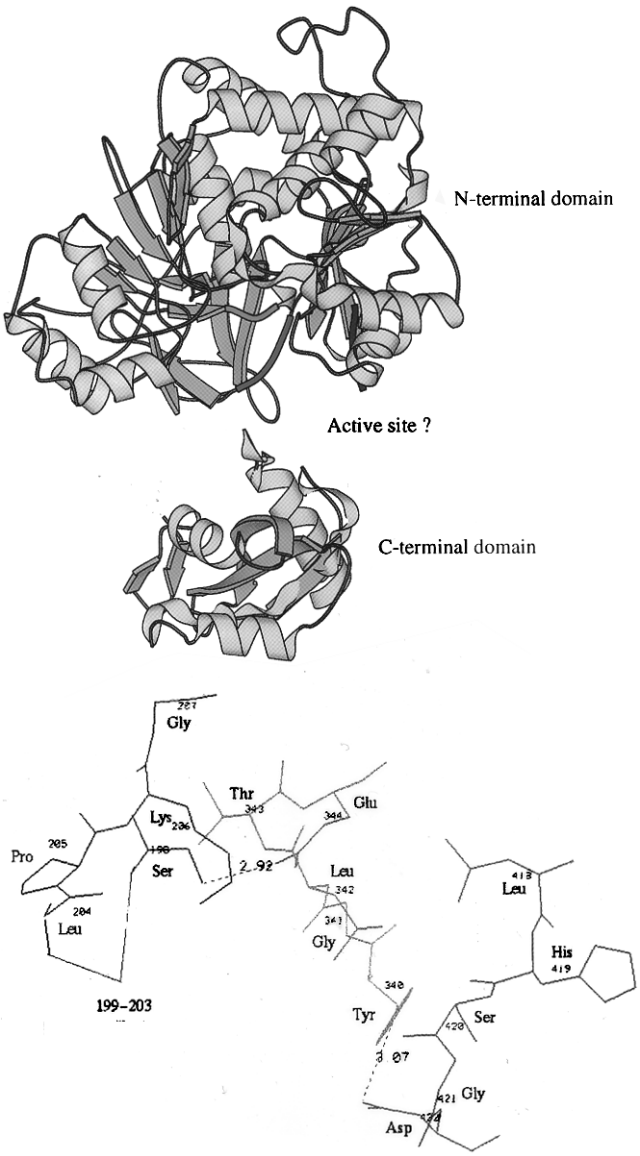

FIGURE 5: IIlustration of the X-ray crystal structure of luciferase from firefly *Photinus pyralis* (*12*). (A) MolScript ribbon diagram representation of backbone structure showing the locations of motif I (blue), motif II (red), and motif III (green). (B) Illustration of the interactions between side chains of the residues of the three motifs.

sequence comprising motifs I, II, and III are close, interacting neighbors within three-dimensional space. The location of these motifs on the same face of the active-site cleft suggests that they may contribute to substrate (luciferin and ATP) binding and/or catalysis.

We imagine that motifs I and II of the 4-CBA:CoA ligase are arranged in a manner similar to that seen in the luciferase structure and that they may also contribute to the enzyme active site. The residues that we have replaced in the 4-CBA: CoA ligase (G163, G166, P168, and K169 of motif I and E306 of motif II) correspond to luciferase residues G200, G203, P205, K206, and E344 (see Figure 5B). The transient kinetic data measured for the 4-CBA:CoA ligase mutants (discussed above) indicates that motifs I and II may function primarily in acyl-adenylate formation. Steady-state kinetic analysis of the ligase E306Q mutant revealed normal values for the ATP and CoA K_m but a high 4-CBA K_m value (Table 1), suggesting a possible role of motif II in binding the carboxylate substrate. The motif I mutants, on the other hand, showed normal CoA K_m values, large ATP K_m values, and elevated 4-CBA K_m values (Table 1). The K_d values for 4-CBA binding to the G163I and KI69M ligase mutants determined by fluorescence titration (Figure 4) are, however, equivalent to that of the wild-type ligase, and thus, the loop may turn out to function primarily in ATP binding.

REFERENCES

1. Dunaway-Mariano, D., and Babbitt, P. C. (1994) *Biodegradation 5*, 259.
2. Scholten, J. D., Chang, K.-H., Babbitt, P. C., Charest, H., Sylvestre, M., and Dunaway-Mariano, D. (1991) *Science 253*, 182.
3. Babbitt, P. C., Kenyon, G., Martin, B. M., Charest, H., Sylvestre, M., Scholten, J. D., Chang, K.-H., Liang, P.-H., and Dunaway-Mariano, D. (1992). *Biochemistry 31*, 5594
4. Chang, K.-H and Dunaway-Mariano, D. (1996) *Biochemistry 35*, 13478.
5. Kleinkauf, H., and von Döhren, H. (1996) *Eur. J. Biochem. 236*, 335.
6. Rhodes, W. C., and McElroy, W. D. (1958) *J. Biol. Chem. 233*, 1528
7. Pazzagli, M. Devine, J. H., Peterson, D. O., and Baldwin, T. O. (1992) *Anal. Biochem. 204*, 315.
8. Bhattacharajee, J. K. (1985) *CRC Crit. Rev. in Microbiol. 12*, 131.
9. Delarue, M. (1995) *Curr. Opin. Struct. Biol. 5*, 48.
10. Rizzi, M., Nessi, C., Mattevi, A., Coda, A., Bolognesi, M., and Galizzi, A. (1996) *EMBO J. 15*, 5125.
11. Fulda, M., Heinz, E., and Wolter, F. P. (1994) *Mol. Gen. Genet. 242*, 241.
12. Conti, E., Franks, N. P., and Brick, P. (1996) *Structure 4*, 287.
13. Sambrook, J., Fritsch, E. F., and Maniatis, T. (1989) *Molecular Cloning: A Laboratory Manual* (2nd ed.). Cold Spring Harbor Laboratory, Cold Spring Harbor, NY.
14. Sanger, F., Nicklen, S., and Coulson, A. R. (1977) *Proc. Nat. Acad. Sci. 74*, 5463.
15. Tabor, S., and Richardson, C. C. (1987) *Proc. Nat. Acad. Sci. 84*, 4767.
16. Lowry, O. H., Rosebrough, N. J., Farr, A. L., and Randall, R. J. (1951) *J. Biol. Chem. 193*, 265.
17. Laemmli, U. K. (1970) *Nature (London) 227*, 680.
18. Chang, K.-H., Liang, P.-H., Beck, W., Scholten, J. D., and Dunaway-Mariano, D. (1992) *Biochemistry 31*, 5605.
19. Taylor, J. W., Ott, J., and Eckstein, F. (1985) *Nucleic Acids Res. 13*, 8765.
20. Cleland, W. W. (1979) *Methods Enzymol. 63*, 103.
21. Ohnishi, M., Yamashita, T., and Hiromi, K. (1977) *J. Biochem (Tokyo) 81*, 99.
22. Mullis, K. B., and Faloona, F. A. (1987) *Methods Enzymol. 155*, 335.
23. Saito, M., Hori, K., Kurotsu, T., Kanda, M., and Saito, Y. (1995) *J. Biochem. (Tokyo) 117*, 276.
24. Gocht, M., and Maraheil (1994) *J. Bacteriol. 176*, 2654.
25. Saraste, M., Sibbald, P. R., and Wittinghofer, A. (1990) *Trends Biochem. Sci. 15*, 430.
26. Schulz, G. E. (1992) *Curr. Opin. Struct. Biol. 155*, 183.
27. Lai, S. Y. (1996) Ph.D. Thesis, University of Maryland, College Park, MD.
28. Schmitz, A., Gartemann, K.-H., Fiedler, J. Grund, E., and Eichenlaub (1992) *Appl. Environ. Microbiol. 58*, 4068.
29. Lozoya, E., Hoffman, H., Douglas, C., Schulz, W., Scheel, D., and Hahlbrock, K. (1988) *Eur. J. Biochem. 176*, 661.
30. Gibson, J., Dispensa, M., Fogg, G. C., Evans, D. T., and Harwood, C. S. (1994) *J. Bacteriol. 176*, 634.
31. Connerton, I. F., Fincham, J. R. S., Sandeman, R. A., and Hynes, M. J. (1990) *Mol. Microbiol. 4*, 451.
32. Van Beilen, J. B., Eggink, G., Enequist, H., Box, R., and Winholt, B. (1992) *Mol. Microbiol. 6*, 3121.
33. Mallonee, D. H., White, W. B., and Hylemon, P. B. (1990) *J. Bacteriol. 172*, 7011.
34. Hori, K., Yamamoto, Y., Tokita, K., Saito, F., Kurotsu, T., Kanda, M., Okamura, K., Furuyama, J., and Saito, Y. (1991) *J. Biochem. (Tokyo) 110*, 111.

35. Staab, J. F., Elkins, M. F., and Earhart, C. F. (1989) *FEMS Microbiol. Lett. 59*, 15.
36. Liyanage, H., Penfold, C., Turner, J., and Bender, C. L. (1995) *Gene 153*, 17.
37. Haese, A., Schubert, M., Hermann, M., and Zocher, R. (1993) *Mol. Microbiol. 7*, 905.
38. Farrell, D. H., Mikesell, P., Actis, L. A., and Crossa, J. H. (1990) *Gene* 86, 45.
39. DeWet, J. R., Wood, K. V., Deluca, M, Haelinski, D. R., and Subramani, S. (1987) *Mol. Cell Biol. 7*, 725.
40. Wood, K. V., Lam, Y. A., Sleiger, H. H., and McElroy, W. D. (1989) *Science 244*, 700.
41. Morris, M. E., and Jinks-Robertson, S. (1990) *Gene 98*, 141.

BI971262P